

Molecular dynamics nanoindentation simulation of an energetic material

Yi-Chun Chen, Ken-ichi Nomura,^{a)} Rajiv K. Kalia, Aiichiro Nakano, and Priya Vashishta
*Collaboratory for Advanced Computing and Simulations, University of Southern California,
 Los Angeles, California 90089-0242, USA*

(Received 12 August 2008; accepted 6 October 2008; published online 29 October 2008)

Molecular dynamics simulation approach is used to study nanoindentation of the (100) crystal surface of cyclotrimethylenetrinitramine (RDX) by a diamond indenter. The indenter and substrate atoms interact via reactive force fields. Nanoindentation causes significant heating of the RDX substrate in the proximity of the indenter, resulting in the release of molecular fragments and subsequent “walking” motion of these molecules on the indenter surfaces. © 2008 American Institute of Physics. [DOI: 10.1063/1.3006428]

Over the past two decades, research on energetic materials has focused on structural properties,¹ defects,^{2–4} decomposition, combustion, and detonation chemistry.^{5,6} Indentation experiments have been performed to study structural characteristics and chemical decomposition⁷ of energetic materials.^{7–11} Armstrong and Elban⁸ investigated the role of dislocations in fracture of cyclotrimethylenetrinitramine (RDX) crystals. Their microindentation experiment reveals temperature enhancement due to dislocation pileup and a well-localized damage zone of cracks that cannot propagate because the orthorhombic crystal structure of RDX offers intrinsic resistance to dislocation motion.

It has been shown that the hardness of a material varies with the indenter size. At the submicron level, nanoindentation has become a highly effective tool in exploring fundamental materials physics. High resolution load-displacement data obtained with atomic force microscopy measurements of contact area can provide valuable insights into the onset of dislocation processes, shear instabilities, and phase transformations.

In this letter, we report molecular dynamics (MD) simulation of nanoindentation of the RDX (100) crystal surface. The RDX unit cell is orthorhombic and contains eight covalently bonded $[\text{CH}_2\text{N}(\text{NO}_2)]_3$ molecules.^{9,11} In the simulation, the RDX substrate contains 133 056 atoms in a MD cell of volume of $127.26 \times 128.52 \times 99.08 \text{ \AA}^3$. Periodic boundary conditions are applied in the plane of the substrate. The diamond indenter is constructed by removing atoms from the (111) surface and passivating dangling atoms with hydrogen atoms. The pyramidal shape diamond indenter contains 43 342 atoms and its dimensions are $108.37 \times 108.37 \times 88.66 \text{ \AA}^3$. In our simulation, the indenter and substrate atoms interact via reactive force fields whose parameters were optimized through comparison with quantum mechanical calculations and validated against various experiments.^{12,13}

In the simulation, the indenter and RDX substrate are first relaxed for 11 ps and then their energies are minimized. Atoms close to the bottom layer of the RDX substrate (within 2 nm) are frozen. The initial temperature of the rest of the substrate and the indenter is 150 K. The indenter depth in the substrate is increased in steps of 5 Å over 2.5 ps and then the indenter and substrate are relaxed for 1.5 ps. [The simulation time step is 0.15 fs, and the effective indentation

speed is about 2% of the sound speed in RDX¹⁴ (2.78 km/s).]

The simulation reveals significant heating under the indenter. The temperature distributions at various indentation depths (from 5.2 to 31.6 Å) are shown in Fig. 1. (Here the temperature is calculated from the kinetic energy of atoms averaged over 0.15 ps.) Initially, the RDX substrate directly under the diamond indenter deforms without any significant increase in the thermal energy. When the indentation depth exceeds 10 Å, the temperature of the contact region in RDX rises dramatically due to the conversion of the plastic deformation energy into heat. As the indentation depth increases, the indentation impression grows and the substrate molecules around and underneath the indenter heat up. The temperature in the damage zone is at least 200 K higher than in the rest of the sample. There is a limited amount of pileup, and the RDX molecules display translational and rotational motions. Outside the deformed region, the RDX substrate retains its original crystal structure. Hardness is calculated from the ratio of the applied load to the projected area of the residual impression. At small indentation depths, the calculated value of the hardness is 391 MPa, which compares favorably with the experimental value (between 313.6 and 431.2 MPa). As the indentation size increases, the MD value of hardness drops because of the growth of the plastic deformation region in the RDX substrate.

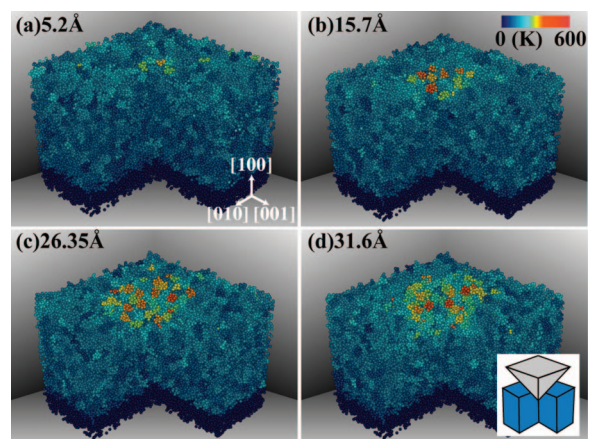


FIG. 1. (Color) Temperature distributions in the RDX substrate at different indentation depths. (a) At 5.2 Å, hardly any heating is observed. (b) At 15.7 Å, the temperature of some of the molecules exceeds 500 K. At indentation depths of (c) 26.35 Å and (d) 31.6 Å, we observe “hot” RDX molecules within $\sim 10 \text{ \AA}$ from the indenter. The inset shows the RDX substrate (blue) and the indenter (gray) schematically.

^{a)}Electronic mail: knomura@usc.edu.

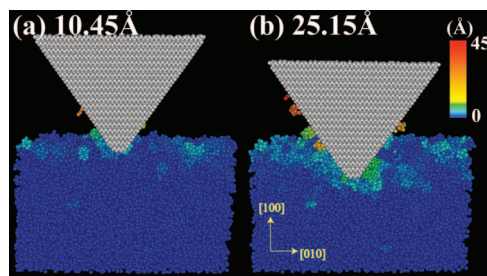


FIG. 2. (Color) Magnitude of the center-of-mass displacement $|\bar{r}_{\Delta c.m.}|$ of RDX molecules. For clarity, only half of the system is shown. Panels (a) and (b) are snapshots of $|\bar{r}_{\Delta c.m.}|$ at indentation depths of 10.45 and 25.15 Å, respectively.

For a RDX molecule, the dipole moment \vec{d} is calculated from $\vec{d} = \sum_{i=1}^{21} q_i (\vec{r}_i - \vec{r}_{c.m.})$, where q_i is the charge of atom i , \vec{r}_i is the atomic position, and $\vec{r}_{c.m.}$ is the center of mass of the molecule. The negatively charged oxygen atoms and positively charged hydrogen atoms contribute to the orientation of the RDX dipole moment, which is perpendicular to the C_3N_3 ring and points inward from the NO_2 group. The RDX molecules with the excess energy tend to rotate until their dipole moments point away from the indenter. The hydrogen atoms on the surface of the indenter attract oxygen atoms in the RDX molecules, causing the oxygen atoms to orient towards the indenter surface.

To study the dynamics of the RDX molecules affected by nanoindentation, we calculate the magnitude of the center-of-mass displacement: $|\bar{r}_{\Delta c.m.}| = |[\sum_{i=1}^{21} m_i \vec{r}_i(t) - \sum_{i=1}^{21} m_i \vec{r}_i(0)] / \sum_{i=1}^{21} m_i|$. Figure 2 shows $|\bar{r}_{\Delta c.m.}|$ at two indentation depths. Initially, there is hardly any change in $|\bar{r}_{\Delta c.m.}|$ [see Fig. 2(a)]. However, $|\bar{r}_{\Delta c.m.}|$ increases dramatically with the indentation depth; see Fig. 2(b). Large values of $|\bar{r}_{\Delta c.m.}|$ are found close to the indenter surface and the RDX molecules move along the indenter surface.

We find that changes in the center of mass are mostly in the $[\bar{1}20]$ direction (see Fig. 3), where the slip is apparent at the maximum indentation depth. Figure 3(b) is a schematic view of the displaced molecules. For clarity, only their centers of mass are shown. Molecules above the (210) plane migrate more than 5 Å from their original positions, but those below the (210) plane hardly move at all.

The simulation also reveals that in order to release the mechanical stress, the RDX molecules “walk” on the indenter surface; see Figs. 4(a) and 4(b). The dynamics of these molecules is a combination of translational and rota-

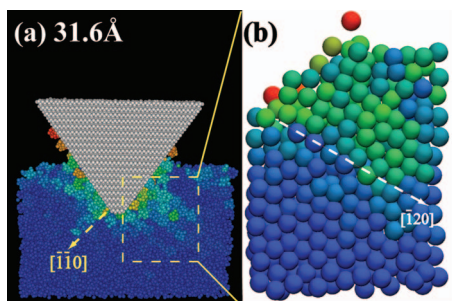


FIG. 3. (Color) Panel (a) shows that the indentation damage is localized in the yellow dashed region. Panel (b) illustrates how the molecules in that region are displaced. Each sphere represents a RDX molecule.

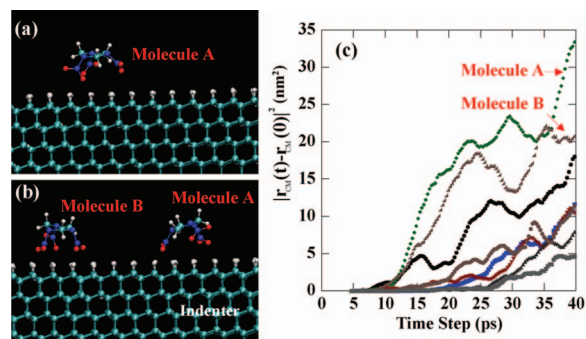


FIG. 4. (Color) (a) and (b) show RDX molecules (A and B) on the indenter surface at 14.5 and 19.65 ps. Red, dark blue, light blue, and white spheres represent oxygen, nitrogen, carbon, and hydrogen atoms, respectively. Panel (c) shows the time dependence of the mean square displacements for a few RDX molecules, including those of molecules A and B.

tional motions, which are reflected in the mean square displacement of molecules as a function of time [see Fig. 4(c)]. This dynamic behavior is similar to 9,10-dithioanthracene and 9-thioanthracene molecules walking on a copper surface.^{15,16}

In summary, our MD simulation reveals dramatic heating and decomposition of RDX molecules from the substrate. Molecular heating and the released RDX molecules are well localized in a damage zone around the indenter. The RDX substrate outside the damage zone remains intact. Our analysis reveals that molecules undergo both translational and rotational motions on the indenter surfaces and that the maximum displacement of RDX molecules is in the (210) plane.

This work was partially supported by ARO-MURI, DTRA, DOE, and NSF. Simulations were performed at the University of Southern California using the 5472-processor Linux cluster at the Research Computing Facility and the 2048-processor Linux clusters at the Collaboratory for Advanced Computing and Simulations.

¹*Structure and Properties of Energetic Materials*, edited by D. H. Liebenberg, R. W. Armstrong, and J. J. Gilman (Materials Research Society, Pittsburgh, 1993), Vol. 296.

²R. W. Armstrong, *J. Phys. IV* **5**, 89 (1995).

³R. W. Armstrong, H. L. Ammon, W. L. Elban, and D. H. Tsai, *Thermochem. Acta* **384**, 303 (2002).

⁴R. W. Armstrong, W. Arnold, and F. J. Zerilli, *Metall. Mater. Trans. A* **38A**, 2605 (2007).

⁵*Decomposition, Combustion, and Detonation Chemistry of Energetic Materials*, edited by T. B. Brill, T. P. Russell, W. C. Tao, and R. B. Wardle (Materials Research Society, Pittsburgh, 1996).

⁶P. J. Miller, C. S. Coffey, and V. F. Devost, *J. Appl. Phys.* **59**, 913 (1986).

⁷R. W. Armstrong and W. L. Elban, in *Proceedings of the Seventh Symposium (International) on Detonation*, Annapolis, MD, 1981, p. 976.

⁸R. W. Armstrong and W. L. Elban, *Mater. Sci. Eng., A* **111**, 35 (1989).

⁹H. G. Gallagher, P. J. Halfpenny, J. C. Miller, J. N. Sherwood, and D. Tabor, *Philos. Trans. R. Soc. London, Ser. A* **339**, 293 (1992).

¹⁰J. T. Hagan and M. M. Chaudhri, *J. Mater. Sci.* **12**, 1055 (1977).

¹¹P. J. Halfpenny, K. J. Roberts, and J. N. Sherwood, *J. Cryst. Growth* **65**, 524 (1983).

¹²A. C. T. van Duin, S. Dasgupta, F. Lorant, and W. A. Goddard, *J. Phys. Chem. A* **105**, 9396 (2001).

¹³A. Strachan, A. C. T. van Duin, D. Chakraborty, S. Dasgupta, and W. A. Goddard, *Phys. Rev. Lett.* **91**, 098301 (2003).

¹⁴T. R. Gibbs and A. Popolato, *LASL Explosive Property Data*, 1980.

¹⁵K. Y. Kwon, R. Perry, G. Pawin, E. Ulin-Avila, K. Wong, and L. Bartels, *Abstr. Pap. - Am. Chem. Soc.* **229**, U746 (2005).

¹⁶K. Y. Kwon, K. L. Wong, G. Pawin, L. Bartels, S. Stolbov, and T. S. Rahman, *Phys. Rev. Lett.* **95**, 166101 (2005).